

Supporting Information:

Exciton Fine Structure and Lattice Dynamics in InP/ZnSe Core/Shell Quantum Dots

Annalisa Brodu¹, Mariana V. Ballottin², Jonathan Buhot², Elleke J. van Harten¹, Dorian Dupont³, Andrea La Porta⁴, P. Tim Prins¹, Mickael D. Tessier³, Marijn A. M. Versteegh⁵, Val Zwiller⁵, Sara Bals⁴, Zeger Hens³, Freddy T. Rabouw¹, Peter C. M. Christianen², Celso de Mello Donega¹, and Daniel Vanmaekelbergh^{1}*

¹*Debye Institute for Nanomaterials Science, Utrecht University, The Netherlands*

²*High Field Magnet Laboratory, HFML-EMFL, Radboud University, The Netherlands*

³*Physics and Chemistry of Nanostructures, Ghent University, Belgium*

⁴*Electron Microscopy for Materials Research, EMAT, University of Antwerp, Belgium*

⁵*Department of Applied Physics, Royal Institute of Technology (KTH), Stockholm, Sweden*

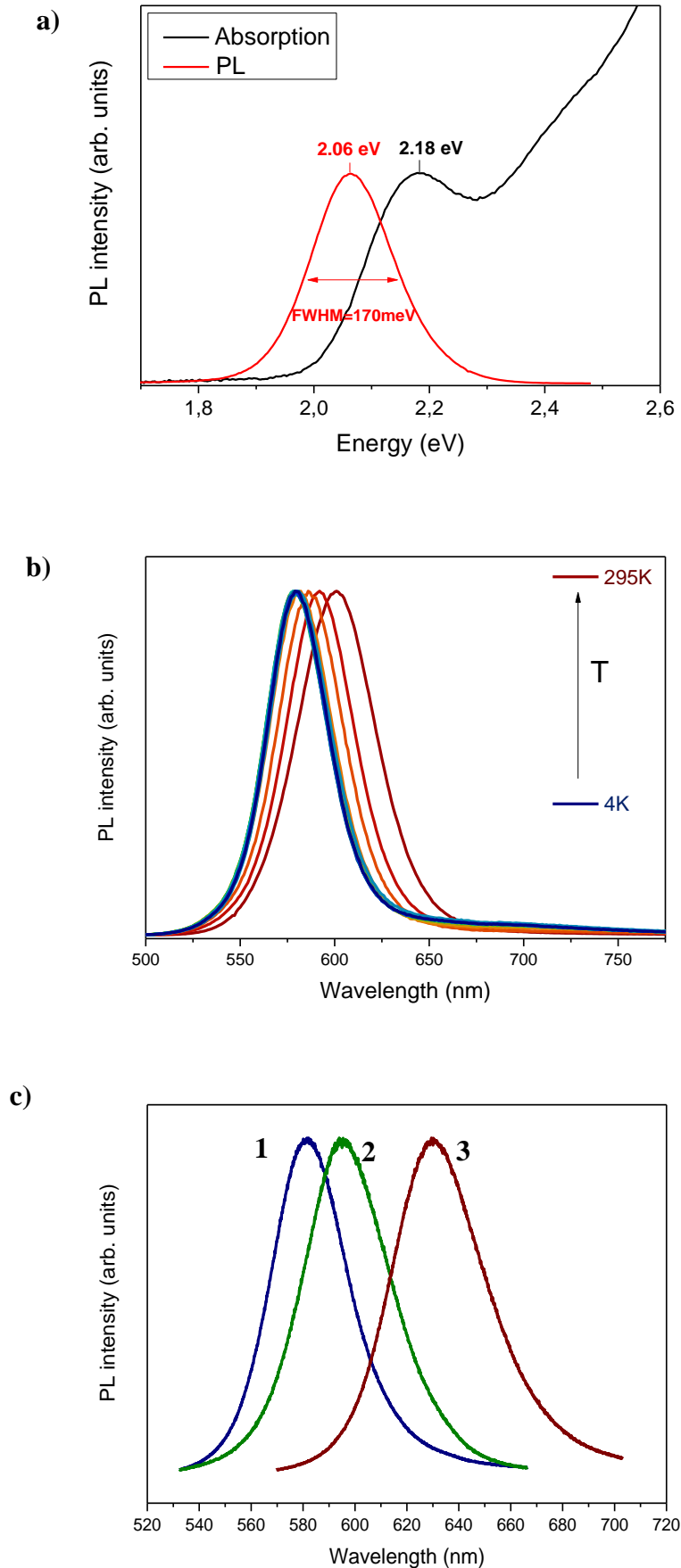


Figure S1: a) Absorption and PL spectra for sample 1 (see S1-c), detected at room temperature. b) PL spectra detected at different temperatures down to 4 K. c) Normalized ensemble PL spectra at low temperature (4 K) of the three InP/ZnSe samples having various core sizes (from 2.9 nm to 3.6 nm).

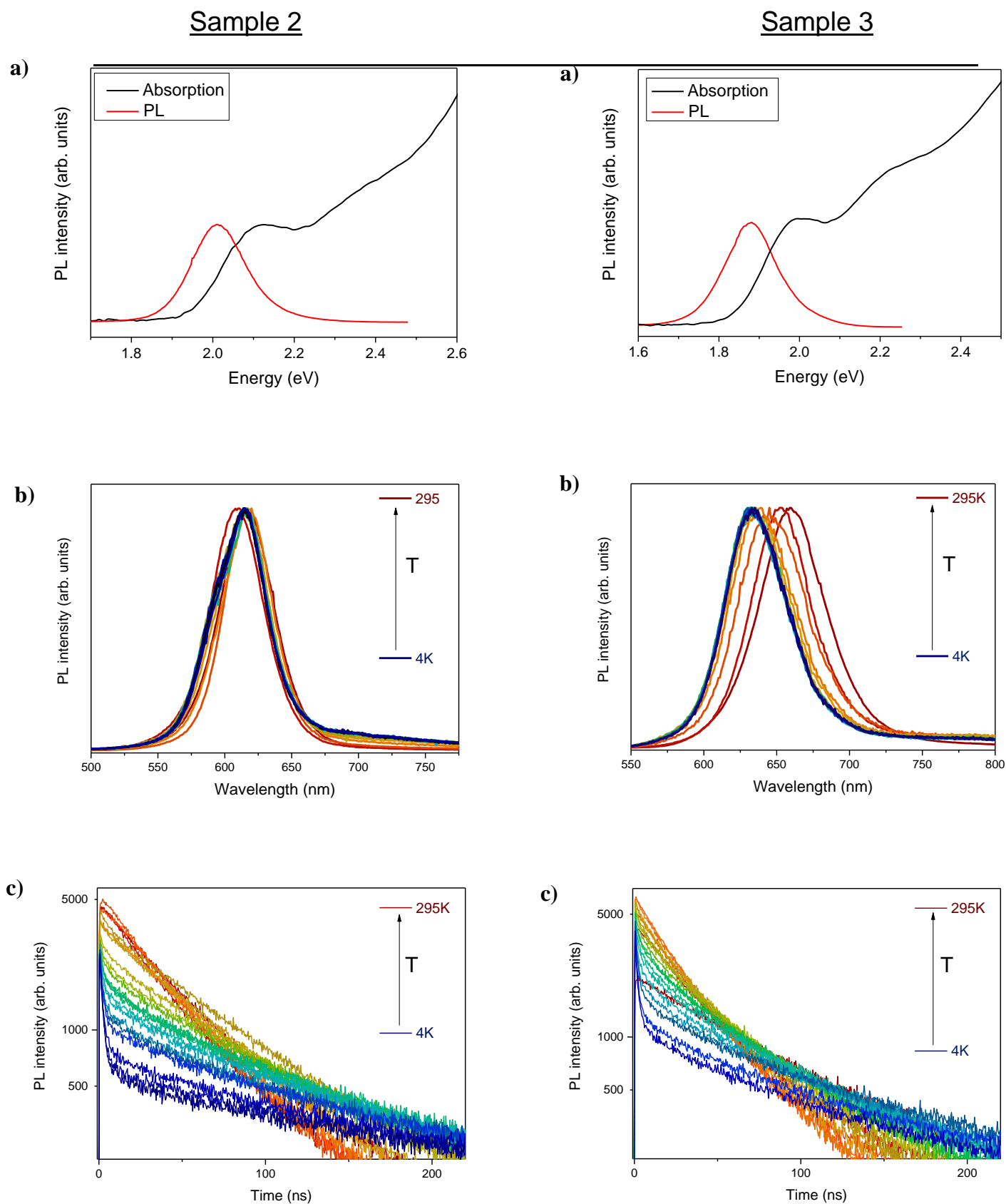
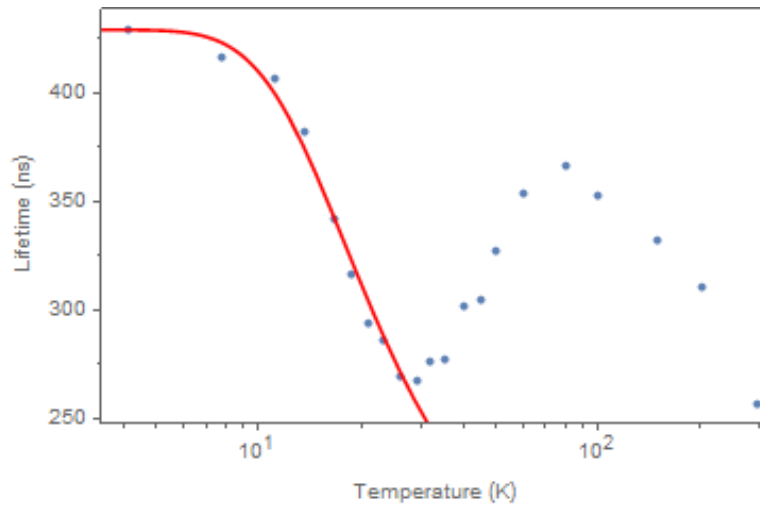
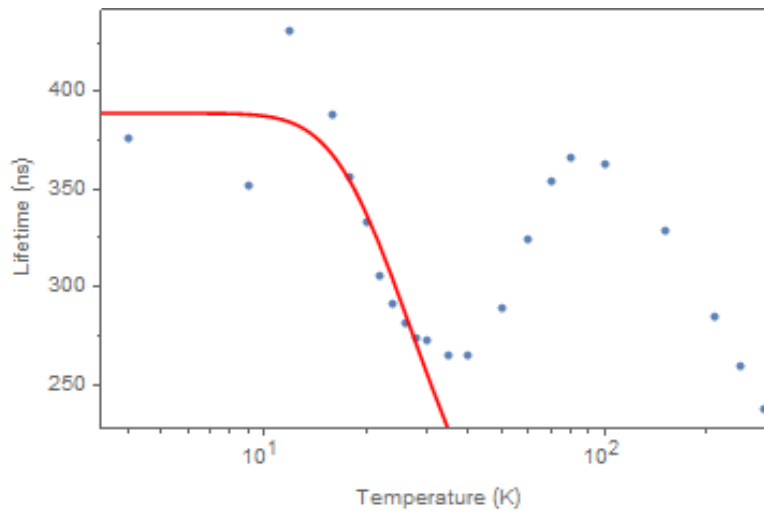


Figure S2: a) Absorption and PL spectra for sample 2 and 3, detected at room temperature. b) PL spectra detected at different temperatures down to 4 K. c) Thermally activated PL decay at zero magnetic field for samples 2 and 3, measured at the PL peak maximum (depending on temperature see Figure S1b), at various temperatures from 4 K (blue) to 295 K (dark red).

Sample 1



Sample 2



Sample 3

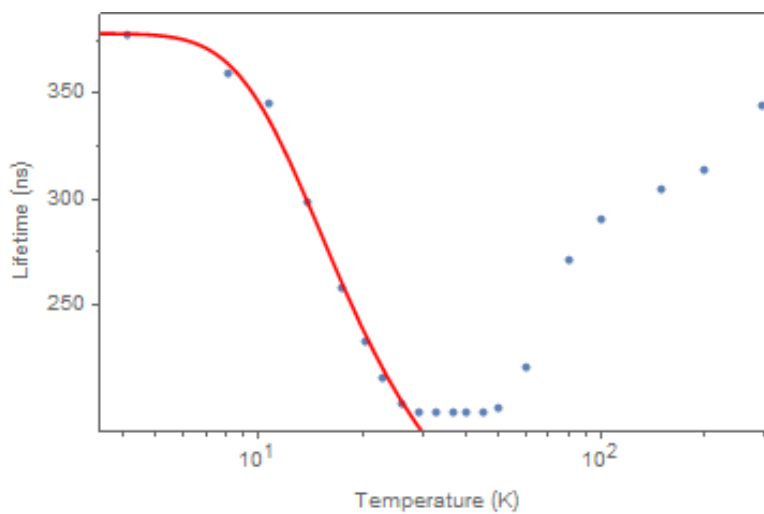


Figure S3: Long component lifetime from a bi-exponential fitting (blue points) of time-resolved PL curves for the three samples and respective fitting (red line) related to the three-level system thermal occupation.

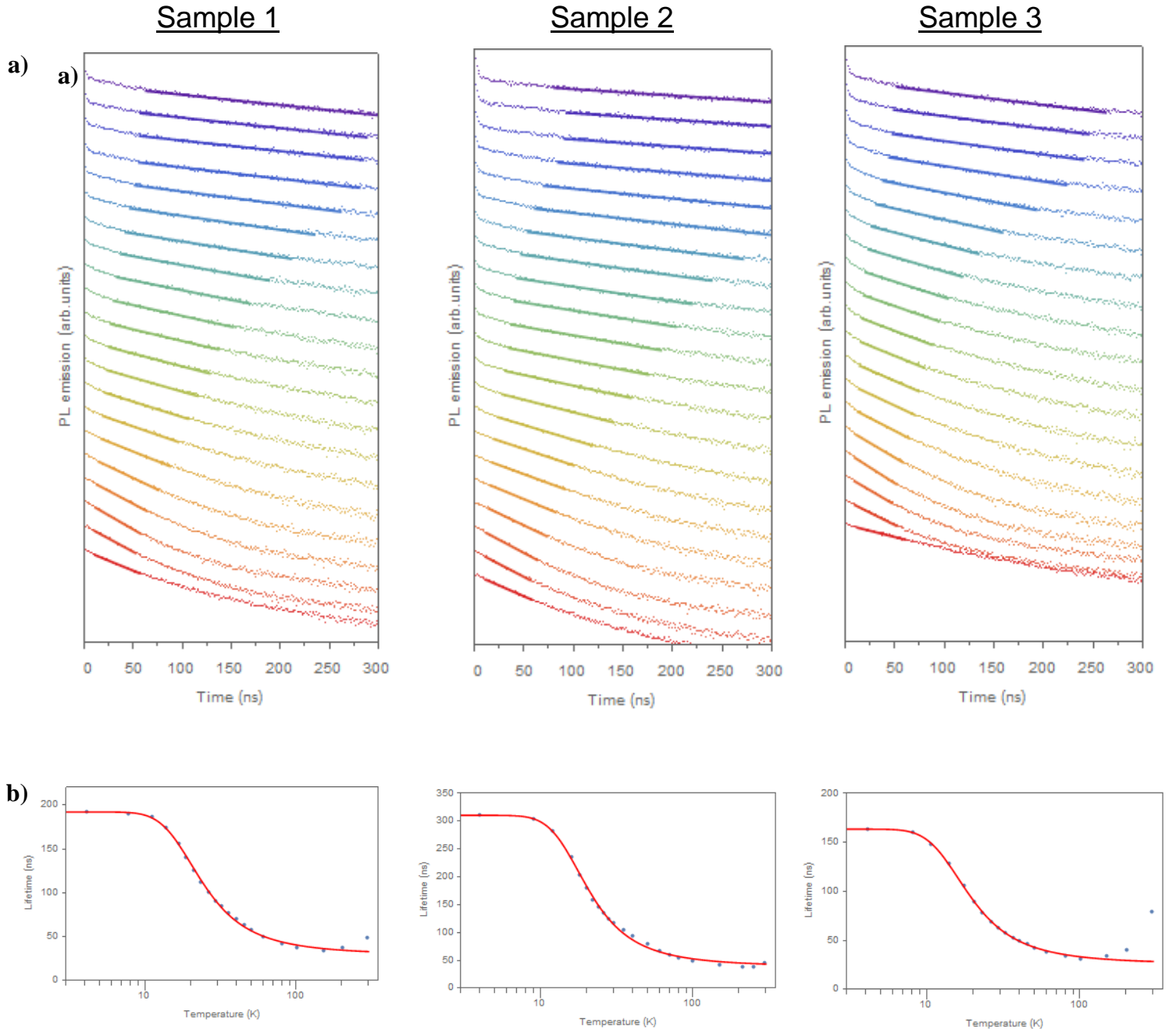


Figure S4: The PL decay curves are very non-exponential. Fast components are presumably due to slow thermalization from the bright state, only prominent at low temperatures. Slow components, resembling power-law decay, may be due to reversible trapping, most prominent at high temperatures. Only the intermediate time range shows the radiative decay of the (dark) exciton state. To determine the decay constant of the radiative component, we fitted single exponential decay to the time range dominated by direct radiative decay. This time range, however, varies with temperature. We started with the data recorded at $T_1 = 4$ K. The lifetime of τ_1 was set as initial parameter then used to define the time range on which the next measurement at $T_2 = 8$ K was fitted. For each measurement at temperature T_{i+1} , the time range considered was determined by the fit results at the next-lower temperature: between $0.3 \tau_i$ and $1.5 \tau_i$. a) PL decay at the peak maximum at various temperatures from 4 K (blue spectrum) to 295 K (red spectrum) for the three samples. For each sample, the solid lines in the figure above show the single-exponential fits, in semi-log representation, exactly on the time range on which they were optimized. b) The exciton lifetime as a function of temperature for the three samples and respective fitting (red line) related to the three-level system thermal occupation. The energy difference between the lowest exciton levels are $\Delta E \sim 5.5$ meV for sample 1, $\Delta E \sim 4.9$ meV for sample 2 and $\Delta E \sim 4.3$ meV for sample 3. Note that when varying the range of the fitting we achieve consistent values.

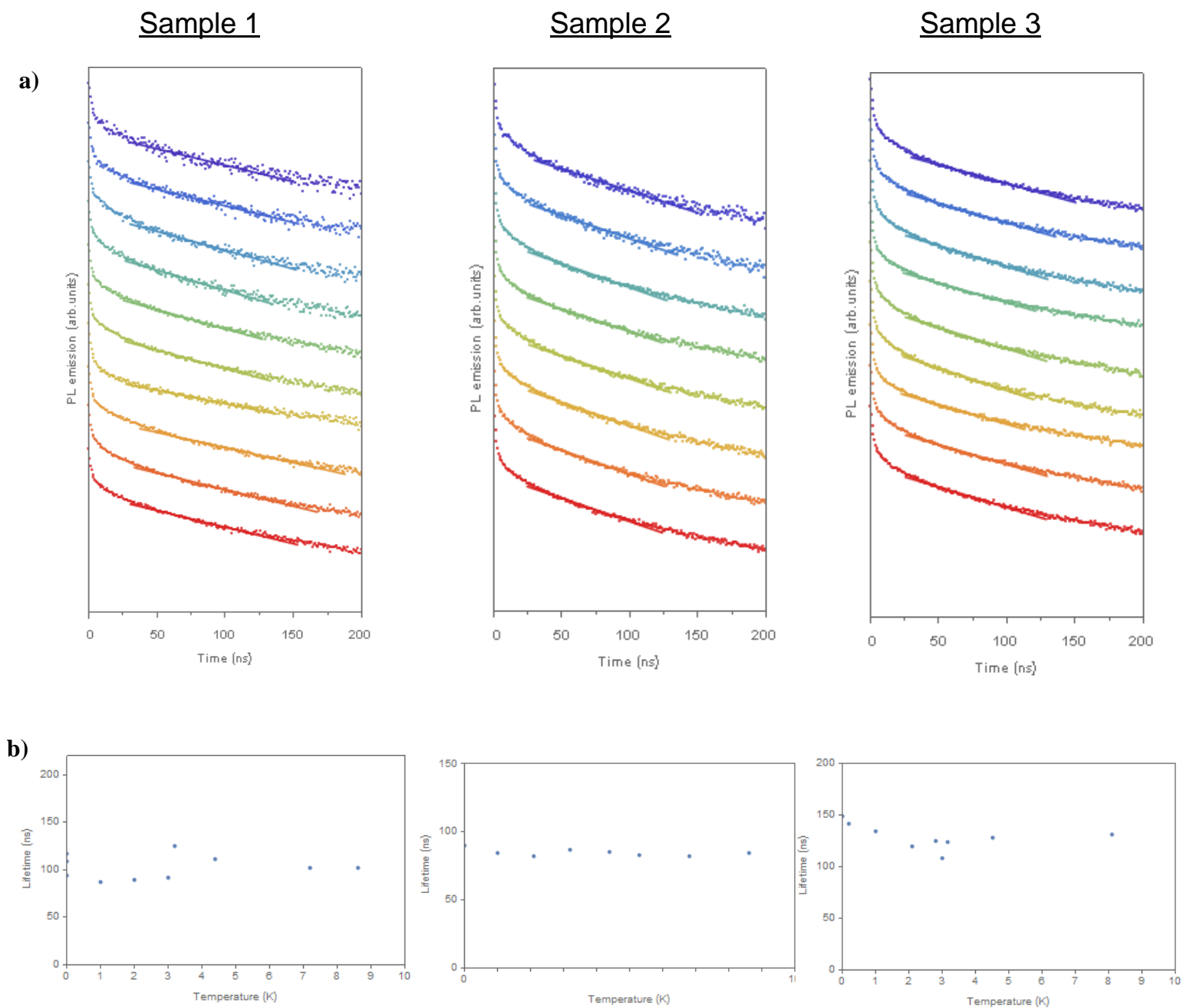


Figure S5: a) PL decay at the peak maximum at various temperatures from 9 K (red spectrum) to 10 mK (blue spectrum) for the three samples. b) Respective long component of the exciton lifetime as a function of temperature calculated as described in figure S4. It remains constant in this range of temperature.

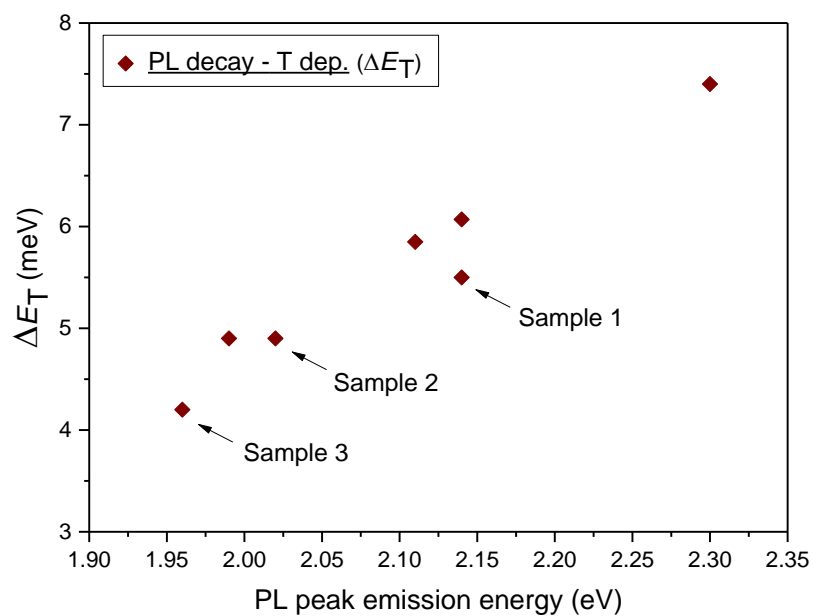


Figure S6: Activation energy obtained from the time-resolved PL decay at varying T . The x -axis displays the monitored PL emission peak-energy.

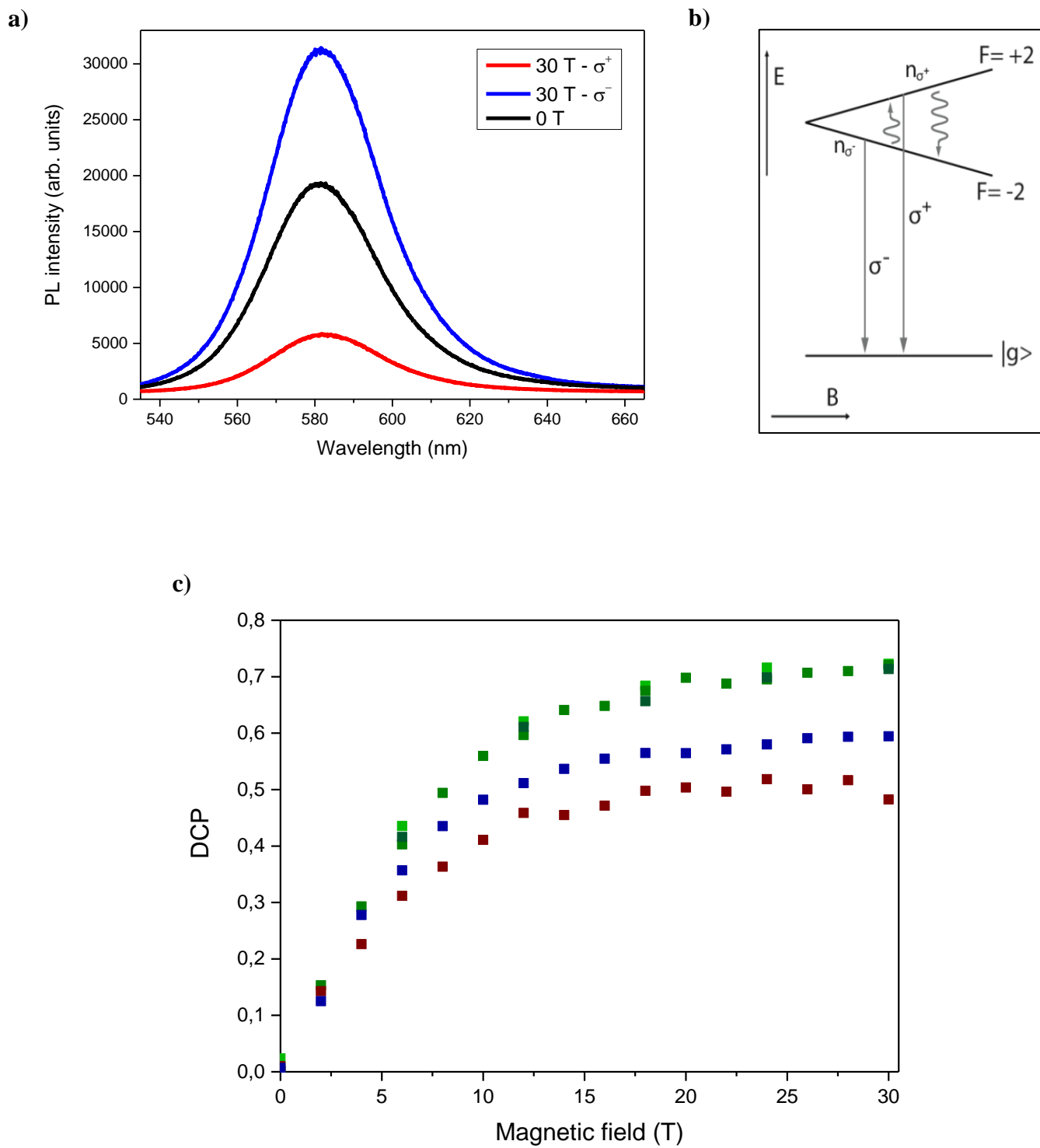


Figure S7: a) PL intensity of right and left circularly polarized emission at 0 T (black) and 30 T (blue and red) of sample 1. b) Exciton energy level scheme and polarized emission due to lifting of the degeneracy of the excitonic level in magnetic field (Zeeman effect). c) Steady-state Degree of Circular Polarization (DCP) at 4 K (green for sample 1, red sample 2, blue sample 3) excited with different polarization: circularly left polarized, circularly right polarized and linearly polarized (different green tonality in sample 1, same trend for the other samples).

Sample 1

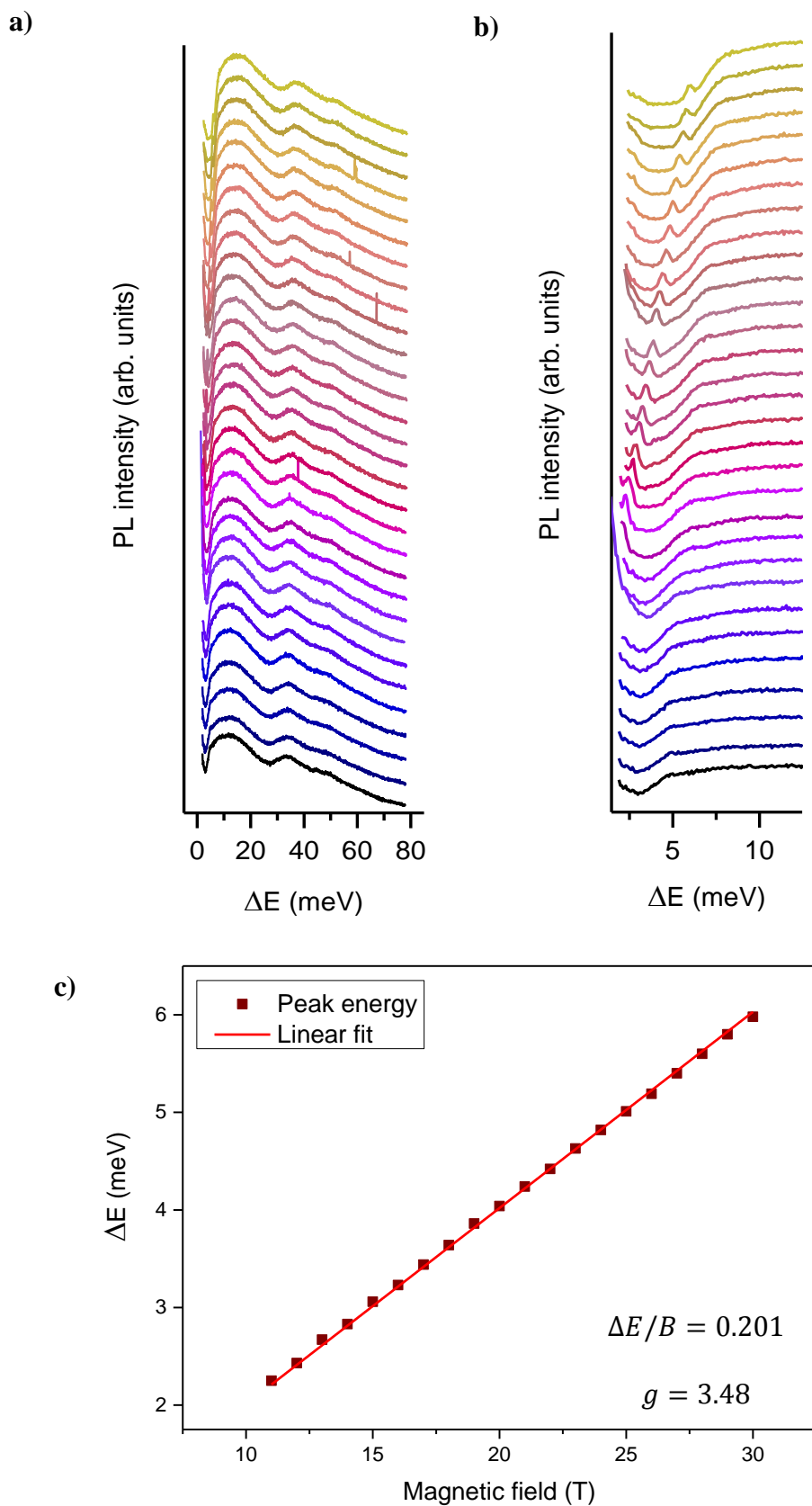


Figure S8: a) FLN spectra at low temperature (4 K) related to sample 1, excited with circular right polarization (σ^+) at 590 nm, at various fields from 0 T to 30 T. b) Zoom-in at low energy that shows fluorescence from the lower Zeeman state after spin flip. The resonantly excited state (2.1 eV) is taken as reference and set to 0 meV. The spectra are vertically shifted for clarity. c) Zeeman splitting of the bright exciton state as a function of applied magnetic field. Linear fitting is shown with solid line, from which we extract the g -factor.

Sample 2

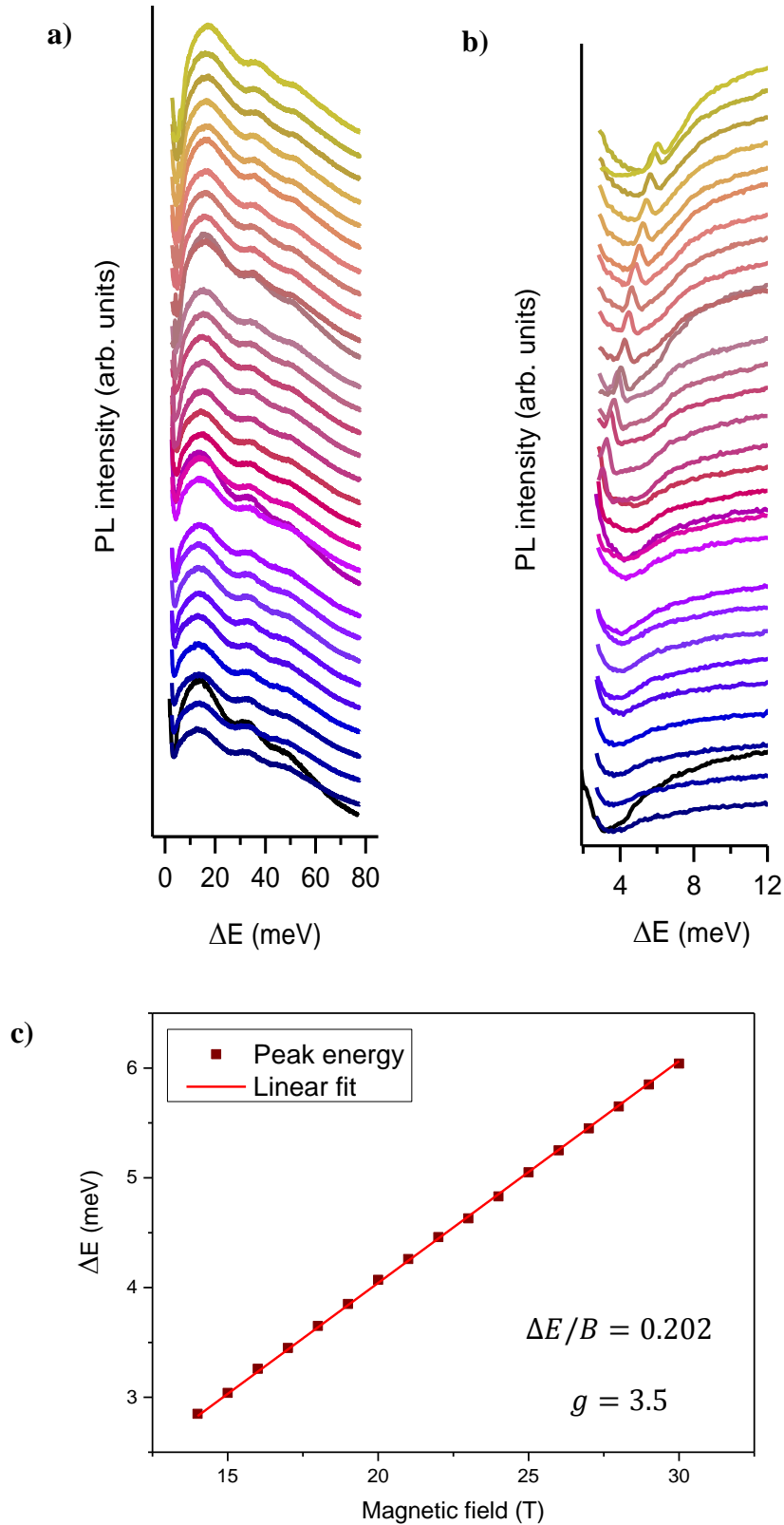


Figure S9: a) FLN spectra at low temperature (4 K) related to sample 2, excited with circular right polarization (σ^+) at 590 nm, at various fields from 0 T to 30 T. b) Zoom-in at low energy that shows fluorescence from the lower Zeeman state after spin flip. The resonantly excited state (2.1 eV) is taken as reference and set to 0 meV. The spectra are vertically shifted for clarity. c) Zeeman splitting of the bright exciton state as a function of applied magnetic field. Linear fitting is shown with solid line, from which we extract the g-factor.

Sample 3

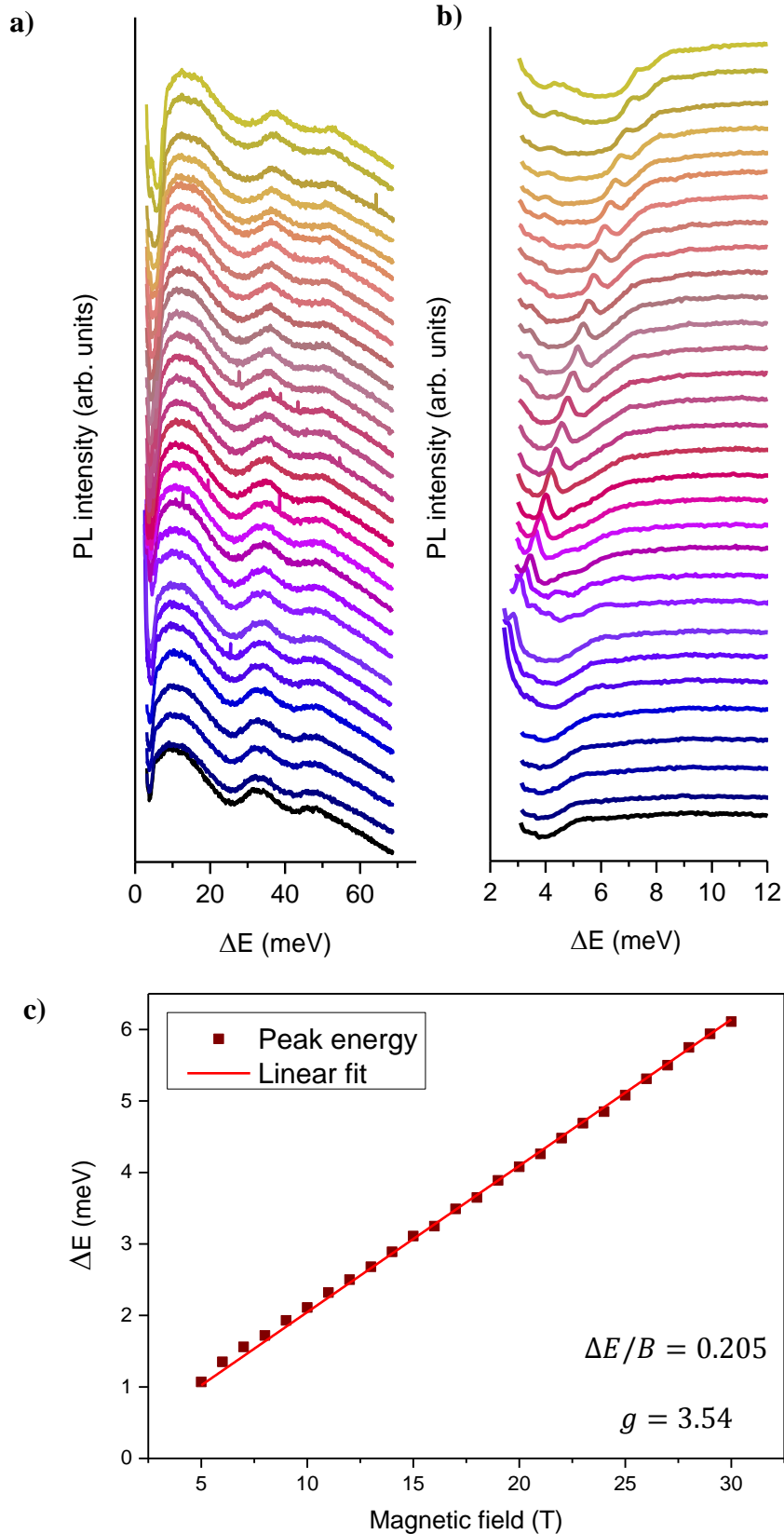


Figure S10: a) FLN spectra at low temperature (4 K) related to sample 3, excited with circular right polarization (σ^+) at 627 nm, at various fields from 0 T to 30 T. b) Zoom-in at low energy that shows fluorescence from the lower Zeeman state after spin flip. The resonantly excited state (2.0 eV) is taken as reference and set to 0 meV. The spectra are vertically shifted for clarity. c) Zeeman splitting of the bright exciton state as a function of applied magnetic field. Linear fitting is shown with solid line, from which we extract the g-factor.

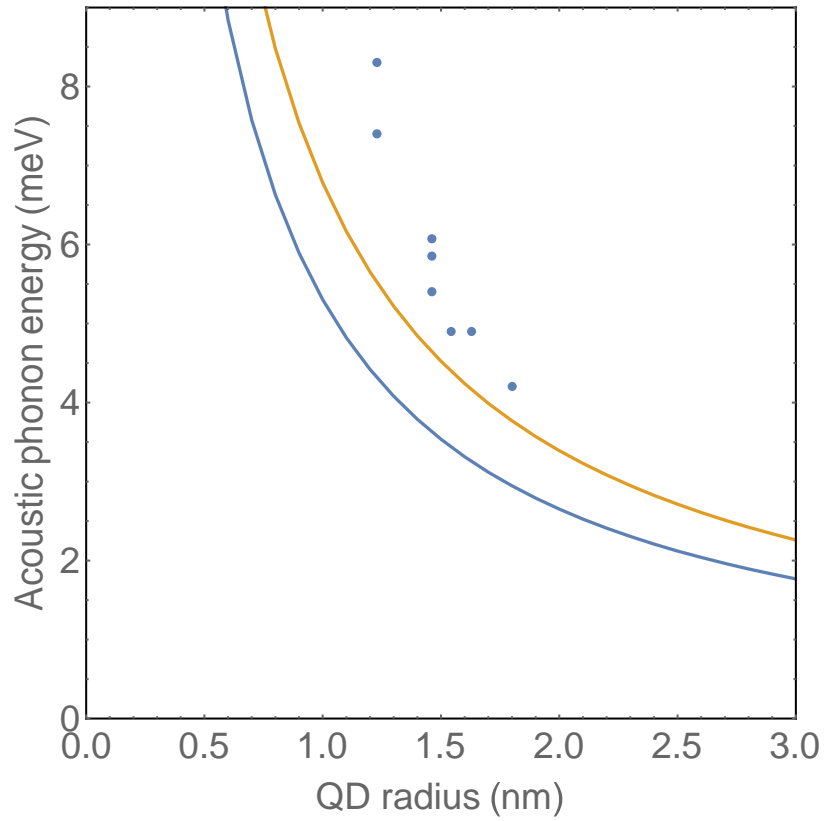


Figure S11: Acoustic-phonon energies from Temperature-dependent lifetime measurements (blue circles) compared with those calculated from Lamb theory for InP hard spheres: orange line is the $l = 0$ mode and blue line is the lowest energy $l = 2$ mode.